

# High-redshift QSOs in the FIRST survey

C.R. Benn,<sup>1</sup>  $\star$  M. Vigotti,<sup>2</sup> M. Pedani,<sup>3</sup> J. Holt,<sup>1,4</sup> K.-H. Mack,<sup>6,2,7</sup> R. Curran,<sup>1,5</sup>  
S.F. Sánchez<sup>1</sup>

<sup>1</sup>*Isaac Newton Group, Apartado 321, 38700 Santa Cruz de La Palma, Spain*

<sup>2</sup>*Istituto di Radioastronomia, CNR, via Gobetti 101, 40129 Bologna, Italy*

<sup>3</sup>*Centro Galileo Galilei, 38700 Santa Cruz de La Palma, Spain*

<sup>4</sup>*Department of Physics & Astronomy, University of Sheffield, Hicks Building, Sheffield S3 7RH, UK*

<sup>5</sup>*Department of Physical Sciences, University of Hertfordshire, College Lane, Hatfield, Herts, AL10 9AB, UK*

<sup>6</sup>*ASTRON/NFRA, Postbus 2, NL-7990 AA Dwingeloo, the Netherlands*

<sup>7</sup>*Radioastronomisches Institut der Universität Bonn, Auf dem Hügel 71, D-53121 Bonn, Germany*

25 October 2018

## ABSTRACT

In a pilot search for high-redshift radio QSOs, we have obtained spectra of 55 FIRST sources ( $S_{1.4\text{GHz}} > 1$  mJy) with very red (O-E > 3) starlike optical identifications. 10 of the candidates are QSOs with redshifts  $3.6 < z < 4.4$  (4 previously known), six with  $z > 4$ . The remaining 45 candidates comprise: a  $z = 2.6$  BAL QSO; 3 low-redshift galaxies with narrow emission lines; 18 probable radio galaxies; and 23 M stars (mainly misidentifications). The success rate (high-redshift QSOs / spectroscopically-observed candidates) for this search is  $1/2$  for  $S_{1.4\text{GHz}} > 10$  mJy, and  $1/9$  for  $S_{1.4\text{GHz}} > 1$  mJy. With an effective search area of  $4030 \text{ deg}^2$ , the surface density of high-redshift ( $z > 4$ ) QSOs discovered with this technique is  $0.0015 \text{ deg}^{-2}$ .

**Key words:** quasars: general - quasars: emission lines - radio continuum: galaxies - early Universe

## 1 INTRODUCTION

Observations of high-redshift ( $z > 4$ ) QSOs strongly constrain models of: the formation and evolution of galaxies and their central black holes (Kauffmann & Haehnelt 2000); the contribution of QSOs to the ionisation of the intergalactic medium at high redshifts (Steidel, Pettini, Adelberger 2001); and, through studies of the Lyman absorption forest, the chemical evolution of the intergalactic medium along the line of sight to the QSO (Rauch 1998, Hamann & Ferland 1999).

Most of the  $\sim 300$   $z > 4$  QSOs now known have been discovered as a result of searches for objects with unusually red optical colours (Fig. 1). A summary of recent searches is given in Table 1. Kennefick et al (1995a, b) searched for objects with unusually red  $g, r, i$  colours in  $340 \text{ deg}^2$  covered by the second Palomar Sky Survey (POSS-II) of the northern hemisphere and discovered 10  $z > 4$  QSOs (see also Djorgovski 2001). Similarly, Sloan Digital Sky Survey (SDSS) commissioning images have been searched for objects with red  $u, g, r, i, z$  colours. More than 100  $z > 3.5$  QSOs have been found so far (Fan et al 2000, 2001; Schneider et al 2001; Zheng et al 2001; Anderson et al 2001, Richards et al 2001),

and this number will rise rapidly as SDSS nears completion ( $\sim 10000 \text{ deg}^2$ ) over the next few years. In the south, Storrie-Lombardi et al (2001) searched UKST plates scanned with the Automated Plate Measuring facility (APM) in Cambridge for objects with  $B_J - R > 2.5$ , and found 49 QSOs with  $z > 4$ .

A disadvantage of the purely optical searches is that complex colour criteria are needed to exclude the much larger number of red stars, which makes it difficult to correct for incompleteness. Alternatively, simple one-colour criteria can be used, but then a large fraction of the high-redshift QSOs is missed (compare in Table 1 the surface densities attained for different types of optical selection). Starting with a sample of radio QSOs allows one to reduce the number of candidates without resorting to complex colour criteria, and is less likely to bias the selection against dusty objects. E.g. Hook et al (1998) sought red objects identified with flat-spectrum QSOs with  $S_{5\text{GHz}} > 25$  mJy over  $1600 \text{ deg}^2$ , and found 6 with  $z > 3$  (none with  $z > 4$ ). Snellen et al (2001) sought red objects identified with flat-spectrum radio sources  $S_{5\text{GHz}} > 30$  mJy in the Cosmic Lens All-Sky Survey (CLASS, Myers et al 2001) over  $6400 \text{ deg}^2$ , and found 4 QSOs with  $z > 4$ , i.e.  $1 z > 4$  QSO per  $1600 \text{ deg}^2$ .

Higher surface densities can be attained by observing the counterparts of fainter radio sources. In this paper we

$\star$  Email: crb@ing.iac.es

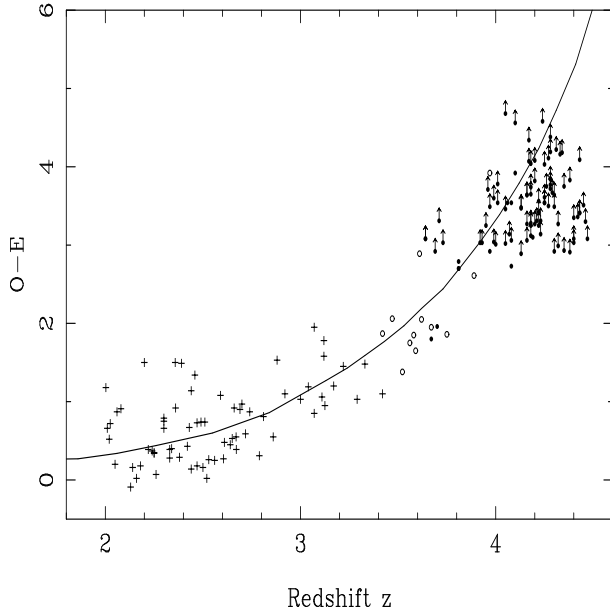


**Figure 1.** The variation of POSSI  $O - E$  colour with redshift, for QSOs from the FIRST bright quasar survey (crosses, White et al 2000), the SDSS and POSSII searches for high-redshift QSOs (spots), and a selection of radio QSOs with  $3.4 < z < 4.0$  from the NASA Extragalactic Database (circles). The QSOs in these samples were selected in part on the basis of colour, but nevertheless trace the typical reddening of a QSO with increasing  $z$  (prediction for typical QSO shown as solid line) as the continuum redward of the  $\text{Ly}\alpha$  line moves out of the observed  $O$  band (red limit  $\approx 5000 \text{ \AA}$ ). As redshift increases above 4.5, the predicted brightness of a QSO in  $E$  band drops sharply, so few are likely to be detected. With the criteria  $O - E > 3$ ,  $E < 18.6$  used here, our QSO search is probably complete for  $z > 4$ , but incomplete for  $3 < z < 4$ .

report on a pilot search for high-redshift QSOs amongst very red,  $O - E > 3$  (see Fig. 1), optical identifications of FIRST radio sources  $S_{1.4\text{GHz}} > 1 \text{ mJy}$  (with no selection on radio spectral index).

There is no overlap between this search and the FIRST bright quasar survey (White et al 2000, Becker et al 2001), whose selection criterion  $O - E < 2$  preclude detection of most high-redshift QSOs (none with  $z > 3.7$  were catalogued), as do the colour selection criteria of most large QSO surveys, e.g. the 2dF QSO survey (Croom et al 2001).

## 2 SAMPLE

The FIRST radio catalogue (White et al 1997) currently includes 722354 sources detected with peak  $S_{1.4\text{GHz}} > 1 \text{ mJy}$  over  $7988 \text{ deg}^2$  ( $\approx 90 \text{ sources deg}^{-2}$ ), mainly  $7 < RA < 17^h$ ,  $-5 < Dec < 57^\circ$ . We sought optical identifications of these sources with objects catalogued by the APM (Irwin et al 1994) on the POSS-I  $O$  (blue) and  $E$  (red) plates. We did not seek optical identifications at the mid-points of likely double radio sources ( $\sim 10\%$  of the catalogue), since this would have required a substantial enlargement of the search area. The colour-magnitude distribution of the star-like optical identifications lying within  $1.5 \text{ arcsec}$  of a FIRST source is shown in Fig. 2. We selected as candidate  $z > 4$  QSOs

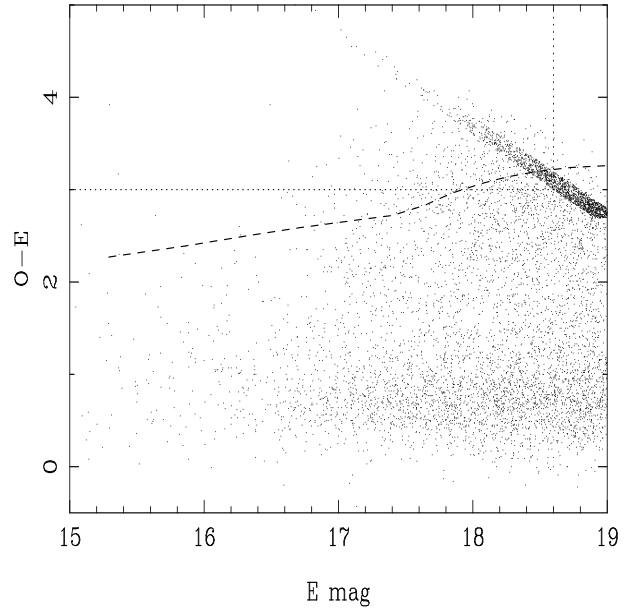


**Figure 2.** Distribution in colour and magnitude of starlike (POSSI/APM) optical identifications of FIRST radio sources. Objects with no  $O$  magnitude have been plotted with  $O - E = 21.7 - E$ , and the  $E$  magnitudes have been randomised  $\pm 0.1$  so that the density of points in this region can be seen. Most of the objects in the lower part of the diagram are true QSOs. Most of those clustered at upper right are misclassified radio galaxies (the dashed line shows the expected colour-magnitude relationship for a redshifted giant elliptical galaxy), and many of the other red objects are misidentifications with galactic M stars. Some may also be BAL QSOs, which tend to be red. The candidate high-redshift QSOs observed here are drawn from the region enclosed by the dotted line.

all starlike optical identifications with  $O - E > 3$  (see Fig. 1) and  $E < 18.6$  (the POSS blue limit is  $O \approx 21.7$ ). Trial spectroscopy showed that  $\sim 80\%$  of these are actually radio galaxies, which greatly outnumber QSOs at  $E \sim 18$ ,  $O - E \sim 3$  (Fig. 2). It was possible to filter out most of these by inspecting images from the digitised POSS-II survey, using the SExtractor program (Bertin & Arnouts 1996) to characterise the relationship between FWHM and intensity for stars (in each image), and thus to distinguish between stellar and extended images. In addition, we filtered out the  $\approx 25\%$  of starlike images for which APM recorded no blue magnitude (i.e. implied magnitude fainter than the blue plate limit), but which were easily visible on the Minnesota APS scans of POSS-I (Pennington et al 1993); these images were missed by APM due to the coarser scanning resolution and greater susceptibility to confusion with nearby images. This selection procedure yielded a total of 109 candidate high-redshift QSOs.

## 3 OBSERVATIONS AND REDUCTION

Spectra were obtained of a random sample of 55 of the 109 candidates with the Isaac Newton Telescope's IDS spectrograph on 2001 Mar 14, and with the Isaac Newton (IDS), William Herschel (ISIS) and Calar Alto 2.2-m (CAFOS) spectrographs on service nights between 2000 March 19 and

**Table 1.** Recent searches for high-redshift QSOs

Search programme	Colour criterion	optical limit	$S_{lim}$ mJy	Area deg <sup>2</sup>	Cands	$z >$	N	$\sigma$ deg <sup>-2</sup>	Hiz / cands	Reference
(1)	(2)	(3)	(4)	(5)	(6)	(7)	(8)	(9)	(10)	(11)
DPOSS-II	gri	$r < 19.6$	—	340	85	4.0	10	0.029	0.11	Kennefick et al 1995a,b
SDSS	ugriz	$i < 20$	—	180		4.0	18	0.10		Fan et al 2001
APM/UKST	$B_J - R > 2.5$	$R < 19.3$	—	8000		4.0	49	0.0061		Storrie-L. et al 2001
INT wide-angle surv.	griz	$r < 24$	—	12.5		4.0	3	0.24		Sharp et al 2001
CLASS flat-spectrum	$O - E > 2$	$E < 19$	$S_5 > 30$	6400	27	4.0	4	0.00063	0.15	Snellen et al 2001
GB/FIRST flat-spec.	$O - E > 1.2$	$E < 19.5$	$S_5 > 25$	1100	50	4.0	0	0.0	0.00	Hook et al 1998
"	$O - E > 1.2$	$E < 19.5$	$S_5 > 25$	1100	50	3.0	6	0.005	0.12	"
FIRST	$O - E > 3$	$E < 18.6$	$S_{1.4} > 1$	4030	55	4.0	6	0.0015	0.11	This paper
"	$O - E > 3$	$E < 18.6$	$S_{1.4} > 10$	4030	9	4.0	4	0.0010	0.44	"

Column 4 gives, where appropriate, the radio flux-density limit  $S_\nu$ , for frequency  $\nu$  in GHz. Column 9 gives the surface density of high-redshift QSOs discovered. Column 10 gives the ratio between the number of high-redshift QSOs found (column 8) and the number of candidates for spectroscopy (column 6).

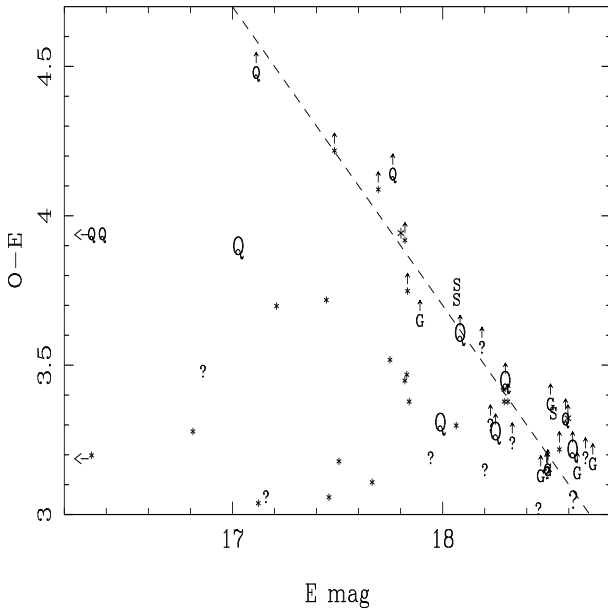


**Figure 3.** Colour-magnitude distribution for the candidate high-redshift QSOs. The symbols for spectral type are as used in Table 2 (Q = QSO, S = narrow-emission-line galaxy, G = radio galaxy, \* = star, ? = probable radio galaxy). Large font indicates  $S_{1.4GHz} > 10$  mJy; small font  $S_{1.4GHz} < 10$  mJy. A nominal POSSI blue plate limit  $O = 21.7$  is indicated by the dashed line. Objects with no  $O$  magnitude have been plotted with  $O - E = 21.7 - E$ , and the  $E$  magnitudes have been randomised  $\pm 0.2$  mag to reduce crowding. The arrows indicate upper or lower limits.

2001 Jan 5 (dates given in Table 2). Apart from 2000 Apr 5, May 12 and 2001 Jan 5, the nights were photometric. The INT IDS spectrograph was used with the R150V grating, yielding spectra with dispersion 6.5 Å/pixel, usually centred at 6500 Å. The WHT ISIS dual-arm spectrograph was used with the R158R and R158B gratings in the red and blue arms respectively (with a dichroic separating the light blue and red of 6100 Å). In the red arm, with a TEK CCD detector, this yielded spectra with dispersion 2.9 Å, usually centred at 7400 Å. In the blue arm, with an EEV CCD, the dispersion was 1.6 Å/pixel, and the spectra were usually centred at 4800 Å. The CAFOS spectrum has dispersion 8.5 Å/pixel.

The images were debiased and flat-fielded, cosmic rays were eliminated, and the spectra were extracted, wavelength-calibrated and intensity-calibrated in the usual way, using the IRAF package. A summary of the observations and results is given in Table 2.

## 4 RESULTS

Spectra showing clear emission or absorption features were classified ‘Q’ (QSO, broad emission lines), ‘S’ (Sy2 or starburst type spectrum, narrow emission lines) or ‘\*’ (spectral features of M star). The remainder have been classified ‘G’ (probable radio galaxy, i.e. giant elliptical), where the characteristic 4000-Å break is detected, otherwise ‘?’. Most of the ‘?’ objects will be radio galaxies, rather than misidentifications with stars, judging from the number of M stars detected, the typical distribution of spectral types at this magnitude, and the magnitude distributions and the distributions on the sky of the ‘?’ and ‘\*’ objects. One of the ‘?’ objects, 1036+42, has a flat SED inconsistent with it being a radio galaxy; it may be a low-redshift QSO ( $z < 2.2$ ). Of the other ‘?’ objects, none has an SED consistent with it being a high-redshift QSO, except perhaps 1120+34 and 1349+38. The redshifts of the high-redshift QSOs were measured from emission lines other than Ly $\alpha$  (because of the asymmetrical absorption), except in the case of 0839+51. The colour-magnitude diagram of the candidates is shown in Fig. 3. The spectra of the high-redshift QSOs are presented in Figs. 4, 5.

We find 10 high-redshift QSOs ( $z > 3.6$ ) out of 55 candidates. These candidates were selected from 109 for the whole FIRST catalogue, covering 7988 deg<sup>2</sup>, so the effective area covered by this search is  $\sim 4030$  deg<sup>2</sup>, i.e. we find 0.0025 high-redshift QSOs deg<sup>-2</sup> with  $z > 3.6$ , or 0.0015 deg<sup>-2</sup> with  $z > 4.0$ . For  $S_{1.4GHz} > 1$  mJy,  $E < 18.6$ , the  $z > 4$  search will be near-complete (Fig. 1). The surface density on the sky is compared with that from other searches for high-redshift QSOs in Table 1. The surface density of  $z > 4$  radio QSOs discovered here is twice as high as that from the Snellen et al search, because of the lower flux-density limit. The efficiency of the search (number of high-redshift QSOs / number of candidates for spectroscopy) is 0.44 for  $S_{1.4GHz} > 10$  mJy, higher than for previous searches, probably because of the careful filtering of the candidates.

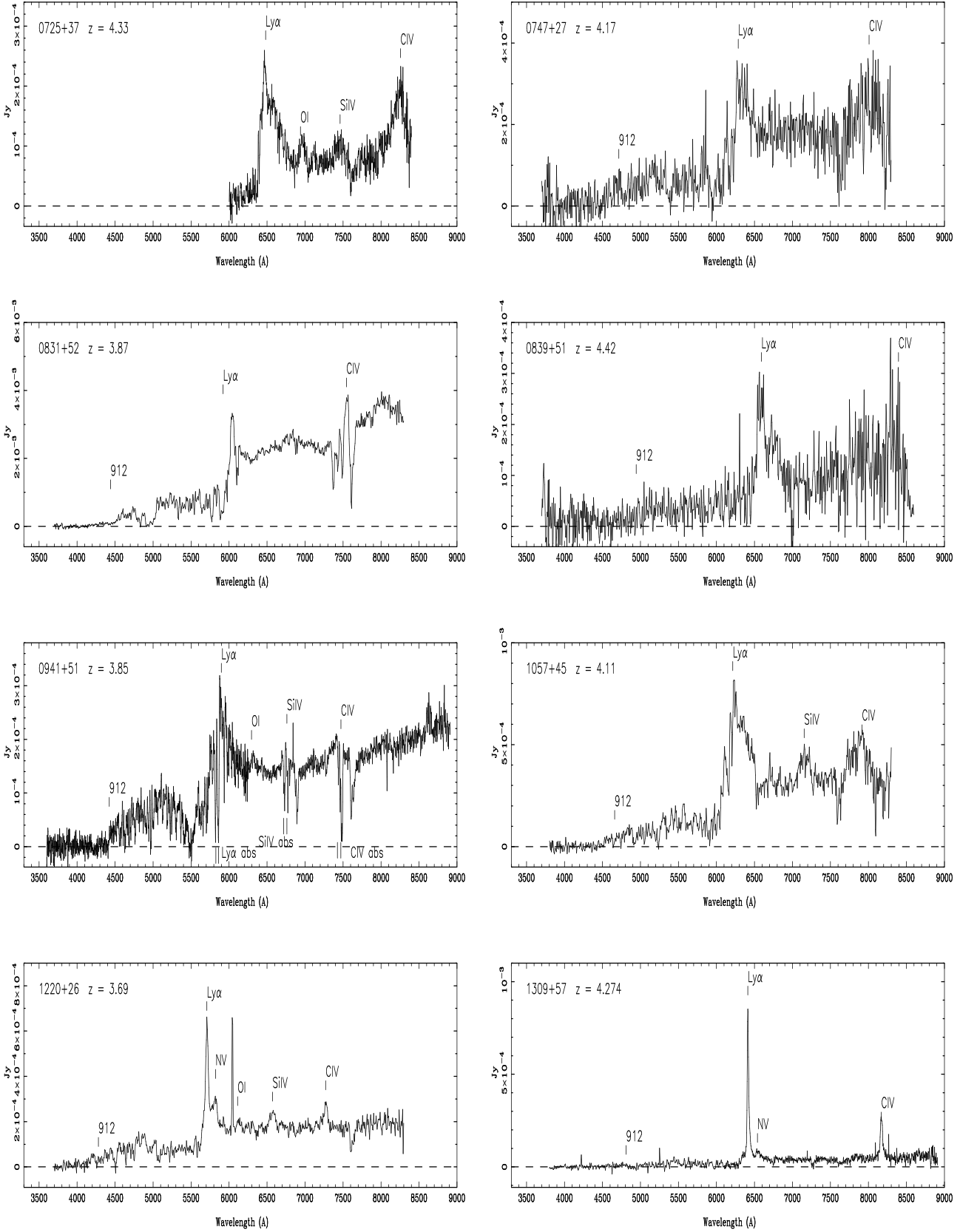


**Figure 4.** Spectra of 8 of the 10 high-redshift QSOs (see Fig 5 for the remainder). Spectral features are labelled at wavelengths corresponding to the quoted redshift, assuming rest-frame wavelengths in Å of 1216 (Ly $\alpha$ ), 1240 (NV), 1302 (OI/SiII blend), 1400 (SiIV/OIV blend), 1549 (CIV). For 0941+51, the metal-line absorption systems at  $z = 3.80, 3.83$  are also indicated. The spectra have not been corrected for the terrestrial atmospheric absorption bands, notably at 7594 and 6867 Å (A and B bands).

**Table 2.** High-redshift QSO candidates

RA J2000 (1)	Dec J2000 (2)	S <sub>1.4</sub> mJy (3)	R-O " (4)	<i>E</i> (5)	<i>O</i> − <i>E</i> (6)	Tel (7)	Date obs. (8)	T sec (9)	ID (10)	<i>z</i> (11)	$\sigma_z$ (12)	Notes (13)
<b>High-redshift QSOs:</b>												
072518.29	370517.9	26.6	0.6	18.3	>3.4	W	010105	900	Q	4.33	.01	
074711.16	273903.6	1.5	0.8	17.2	>4.5	I	010314	200	Q	4.17	.02	
083141.68	524517.1	0.9	0.7	15.3	3.9	I	010314	200	Q	3.87	.03	Irwin et al (1998), <i>z</i> = 3.91
083946.11	511203.0	41.6	0.8	18.5	>3.2	I	010314	300	Q	4.42	.02	Snellen et al (2000), <i>z</i> = 4.41
094119.36	511932.3	2.7	1.3	17.6	>4.1	W	000319	1200	Q	3.85	.01	
105756.27	455553.0	1.4	0.5	16.5	3.9	I	000405	300	Q	4.11	.02	Stern et al (2000), <i>z</i> = 4.12
122027.93	261903.6	35.0	0.4	17.9	3.3	I	010314	1200	Q	3.694	.005	
130940.61	573309.1	11.5	1.1	18.1	>3.6	W	000319	300	Q	4.274	.005	
142308.19	224157.5	35.4	0.9	18.5	>3.2	I	010314	1200	Q	4.316	.005	
151601.55	430931.3	1.5	0.9	18.4	>3.3	I	010314	300	Q	2.590	.005	
163950.51	434003.3	23.8	0.5	17.1	3.9	W	000718	1000	Q	3.99	.015	
<b>Low-redshift QSOs and galaxies:</b>												
091441.31	295621.4	4.8	0.3	18.6	>3.1	I	010314	300	G			
093255.83	353439.1	1.9	0.9	18.2	3.1	I	010314	300	?			
101058.24	283247.0	2.3	0.4	18.6	>3.1	I	010314	100	?			
103549.91	300732.1	9.0	0.3	18.4	3.3	I	010314	300	S	0.587	.002	3727, 5007? blue SED
103647.80	420852.7	2.2	0.4	18.6	>3.1	I	010314	200	?			
104622.91	345436.0	1.0	0.7	18.6	>3.1	I	010314	300	G			
104801.61	260032.3	11.2	0.5	18.6	3.0	I	010314	300	?			
104958.45	411043.4	1.3	0.5	18.0	3.2	I	010314	300	?			
105719.80	342807.0	5.4	0.0	18.1	>3.6	I	010314	300	G			
105750.00	353300.4	2.3	0.7	18.5	>3.2	I	010314	1300	?			
111411.21	293244.4	1.1	1.0	18.0	3.8	I	010314	300	S	0.279	.001	3727 4861 4959 5007 6563
111557.91	352757.1	3.4	1.4	18.5	>3.2	I	010314	300	?			
111707.05	411736.1	0.7	0.8	18.5	>3.2	I	010314	300	G			
112028.10	345829.4	6.5	0.8	18.2	>3.5	I	010314	300	?			possible high-redshift QSO
115230.18	271808.4	4.2	0.4	17.0	3.0	I	010314	300	?			
121532.16	250956.6	1.0	0.7	18.0	3.7	I	010314	300	S	0.282	.001	3727 4861 4959 5007
124450.93	353906.7	1.5	0.2	17.1	3.5	I	000405	300	?			
130604.97	352603.9	1.1	0.9	18.4	3.0	I	010314	300	?			
134951.93	382334.9	1.7	0.4	18.4	>3.3	I	010314	300	?			possible high-redshift QSO
140816.68	352205.8	9.6	1.1	18.4	>3.4	I	010314	300	G			
143749.26	325917.8	1.3	0.7	18.6	>3.1	I	010314	300	G			
<b>M stars:</b>												
072359.95	523949.4	0.8	0.8	17.6	>4.1	I	010314	300	*			
072801.49	380344.2	1.6	0.7	17.3	3.7	I	010314	300	*			
074144.39	333549.3	136.8	0.6	18.4	>3.3	W	010104	400	*			
075127.64	272736.4	1.2	1.2	18.0	>3.7	W	010104	400	*			
084407.26	280740.4	6.2	0.5	17.5	3.0	W	010105	1200	*			
085700.54	275540.0	0.8	0.8	18.5	>3.2	W	010105	400	*			
090556.33	224419.1	2.4	1.5	17.5	>4.2	I	010314	200	*			
091953.76	340906.7	1.2	0.8	17.1	3.0	I	010314	200	*			
100125.11	370629.4	1.1	0.8	16.8	3.2	I	010314	200	*			
105102.41	314914.5	9.0	0.4	17.8	>3.9	I	010314	300	*			
111212.69	431015.5	1.4	0.9	17.2	3.7	C	000512	900	*			
112518.16	495158.8	3.0	1.1	17.8	3.4	I	010314	300	*			
113043.07	514134.1	4.2	0.5	17.7	3.1	I	010314	300	*			
120849.72	392907.1	0.8	1.2	15.3	3.2	I	010314	300	*			
132903.23	323031.5	5.8	1.4	18.1	3.4	I	010314	300	*			
133833.44	531642.1	0.9	0.7	17.9	3.3	I	010314	300	*			
135357.42	343659.7	98.0	1.2	17.8	3.9	I	010314	300	*			
150859.95	271431.0	1.0	0.4	17.9	3.4	I	010314	300	*			
150938.97	434649.8	1.9	0.8	18.4	>3.4	I	010314	300	*			
161150.75	434412.4	1.0	1.0	17.8	3.4	I	010314	300	*			
163535.34	352415.9	5.2	0.6	18.1	3.4	W	000718	300	*			
164217.03	402230.8	6.4	0.2	17.4	3.1	W	000718	300	*			
164401.60	420047.4	4.2	1.2	17.6	3.5	W	000718	300	*			

The columns give: (1-2) right ascension and declination, (3) FIRST 1.4-GHz (integrated, sometimes < peak) flux density, (4) radio - optical displacement, (5-6) APM POSSI *E* magnitude and *O* − *E* colour, (7) telescope with which spectrum obtained (W = William Herschel 4.2-m, I = Isaac Newton 2.5-m, C = Calar Alto 2.2-m), (8) date of observation, (9) exposure time, (10) spectral type (Section 4), (11-12) redshift and rms error on redshift. For low-redshift emission-line objects, the rest-frame wavelengths of detected lines are given in Å in the last column: 3727 OII, 4861 H $\beta$ , 4959/5007 OIII, 6563 H $\alpha$ . For high-redshift QSOs, see Figs. 4, 5.

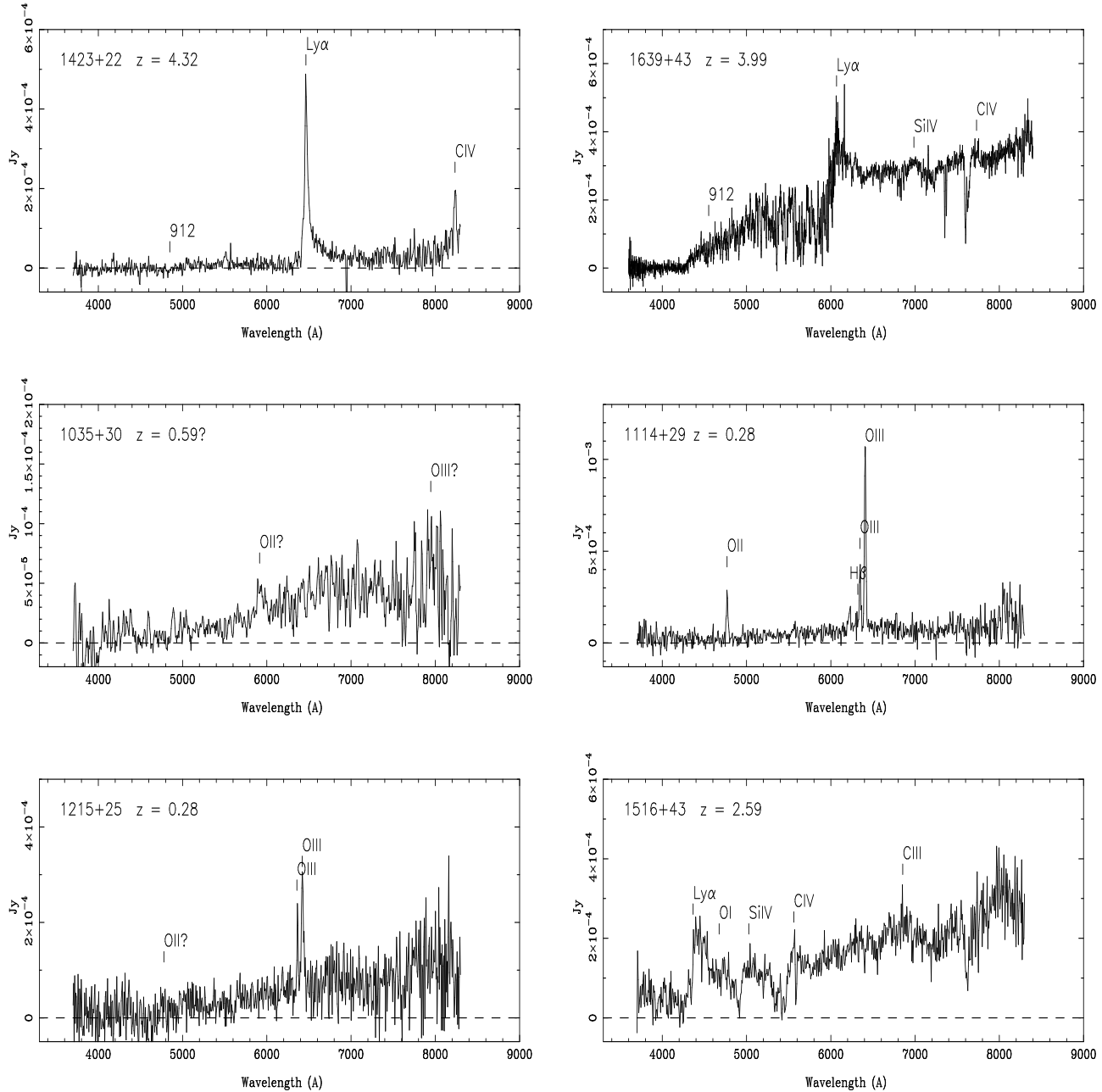


**Figure 5.** Spectra of the two remaining high-redshift QSOs (see caption of Fig. 4); and of 4 other emission-line objects detected in this search (see text). 1516+43 was undetected on the POSS blue plate, but the field is optically confused and its true colour may be bluer than  $O - E = 3$ .

Four of the 10 high-redshift QSOs were previously known: 0747+27 (M. Irwin, private communication), 0831+52 (Irwin et al 1998), 0839+51 (Snellen et al 2001) and 1057+45 (Stern et al 2000). 0831+52 is unusually bright ( $E = 15$ ) and the Ly $\alpha$  forest been studied in detail (Ellison et al 1999). 327-MHz flux densities are available for three of the high-redshift QSOs from the WENSS survey (Rengelink et al 1997). The 0.3 - 1.4-GHz spectral indices  $\alpha$  ( $S_\nu \propto \nu^\alpha$ ) are all flat: -0.1 for 0725+37, 0.0 for 0839+51, and -0.4 for 1639+43. The other 7 QSOs are too faint to be detected in WENSS, or lie below the WENSS declination limit.

The SEDs of the high-redshift radio QSOs reported here

are as varied as those found in optical searches. At least 0941+51 and 0831+52 show metal-line absorption redward of Ly $\alpha$ , probably associated with saturated Ly $\alpha$  lines in the forest. One, 1309+57, shows very narrow Ly $\alpha$  emission, FWHM 20 Å. 1639+43 has almost no Ly $\alpha$  emission, which is unusual (only  $\sim 1/60$  of SDSS QSOs), and it is similar in this respect to the  $z = 4.2$  radio QSO, 0918+06, discovered by Snellen et al. Snellen et al suggested that the unusually strong absorption of the Ly $\alpha$  line might be due to the host galaxy (in both cases this is probably a giant elliptical). A few of the QSOs have probable damped Ly $\alpha$  systems (DLAs, seen in  $\sim 20\%$  of high-redshift QSOs). 0941+51 has a DLA

at  $z = 3.52$ , and this has now been observed at high spectral resolution with WHT ISIS (Centurion et al, in preparation).

The other 45 candidates are a mixed bag (see Magliocchetti et al 2000 for the typical distribution of identification types of all colours at 1 mJy). 1516+43 is a  $z = 2.59$  broad-absorption-line (BAL) QSO with broad, deep SiIV and CIV absorption troughs blueward of the emission features (Fig. 5). 1035+30 (probably), 1114+29 and 1215+25 are low-redshift galaxies exhibiting narrow emission lines (Fig. 5). 18 have SEDs consistent with those of giant elliptical galaxies at  $z \sim 0.3$ . 23 have spectra of late-type M stars. This number is consistent with that expected for chance coincidences, but a few may be true radio stars (Helfand et al 1999 describe a search for counterparts of bright stars in FIRST).

## 5 CONCLUSIONS

We have conducted a pilot search for high-redshift radio QSOs, obtaining optical spectra of 55 FIRST radio sources ( $S_{1.4\text{GHz}} > 1$  mJy) with red (O-E > 3) starlike optical identifications. 10 of the candidates are QSOs with redshifts  $3.6 < z < 4.4$  (4 previously known). Six have  $z > 4$ . The remaining 45 candidates are a mixture of low-redshift galaxies (misclassified as stellar) and M stars (mainly misidentifications). The success rate (high-redshift QSOs / candidates) for this search is 1/2 for  $S_{1.4\text{GHz}} > 10$  mJy, and 1/9 for  $S_{1.4\text{GHz}} > 1$  mJy. With an effective search area of 4030 deg<sup>2</sup>, the surface density of  $z > 4$  QSOs discovered with this technique is 0.0015 deg<sup>-2</sup>.

### Acknowledgments

We are grateful to Alessandro Caccianiga (Observatorio de Lisboa) for taking spectra with the Calar Alto 2.2-m telescope. Rachel Curran and Joanna Holt were 1-year placement students at ING in 1999-2000 and 2000-2001 respectively. KHM was supported by the European Commission, TMR Programme, Research Network Contract ERBFMRXCT96-0034 "CERES". The William Herschel and Isaac Newton Telescopes are operated on the island of La Palma by the Royal Greenwich Observatory in the Spanish Observatorio del Roque de los Muchachos of the Instituto de Astrofísica de Canarias. The Calar Alto observatory is operated by the Max-Planck-Institute for Astronomy, Heidelberg, jointly with the Spanish National Commission for Astronomy. The APS Catalog of POSS I (<http://aps.umn.edu>) is supported by NASA and the University of Minnesota. The NASA/IPAC Extragalactic Database (NED) is operated by the Jet Propulsion Laboratory, California Institute of Technology, under contract with NASA.

## REFERENCES

Anderson S.F. et al, 2001, MNRAS, astro-ph/0103228  
 Becker R.H. et al, 2001, ApJS, astro-ph/0104279  
 Bertin E., Arnouts S., 1996, A&AS, 117, 393  
 Croom S.M., Smith R.J., Boyle B.J., Shanks T., Loaring N.S., Miller L., Lewis I.J., 2001, MNRAS, astro-ph/0104095  
 Djorgovski S.G., 2001, <http://astro.caltech.edu/~george/z4.qsos>  
 Ellison S.L., Lewis G.F., Pettini M., Sargent W.L.W., Chaffee F.H., Foltz C.B., Rauch M., Irwin M.J., 1999, PASP, 111, 946  
 Fan X. et al, 1999, AJ, 118, 1

Fan X. et al, 2001, AJ, 121, in press, astro-ph/0008122  
 Hamann F., Ferland G., 1999, ARA&A, 37, 487  
 Helfand D.J., Schnee S., Becker R.H., White R.L., McMahon R.G., 1999, AJ, 117, 1568  
 Hook I.M., Becker R.H., McMahon R.G., White R.L., 1998, MNRAS, 297, 1115  
 Irwin M.J., Iбата R.A., Lewis G.F., Totten E.J., 1998, ApJ, 505, 529  
 Irwin M.J., McMahon R.G., Maddox S., 1994, Spectrum no. 2., p. 14  
 Kauffmann G., Haehnelt M., 2000, MNRAS, 311, 576  
 Kennefick J.D., de Carvalho R.R., Djorgovski S.G., Wilber M.M., Dickson E.S., Weir N., 1995a, AJ, 110, 78  
 Kennefick J.D., Djorgovski S.G., de Carvalho R.R., 1995b, AJ, 110, 2553  
 Magliocchetti M., Maddox S.J., Wall J.V., Benn C.R., Cotter G., 2000, MNRAS, 318, 1047  
 Myers S.T. et al, 2001, AJ, in press  
 Pennington R.L., Humphreys, R.M., Odewahn, S.C., Zumach, W., Thurmes, P.M., 1993, PASP, 105, 521.  
 Rauch M., 1998, ARA&A, 36, 267  
 Rengelink R.B., Yang T., de Bruyn A.G., Miley G.K., Bremer M.N., Röttgering H.J.A., Bremer M.A.R., 1997, A&AS, 124, 259  
 Richards G.T. et al, 2001, AJ, 121, 2308  
 Schneider D.P. et al, 2001, AJ, 121, in press, astro-ph/0012083  
 Sharp R.G., McMahon R.G., Irwin M.J., Hodgkin S.T., 2001, MNRAS, astro-ph/0103079  
 Snellen I.A.G., McMahon R.G., Dennett-Thorpe J., Jackson N., Mack K.-H., Xanthopoulos E., 2001, MNRAS, in press, astro-ph/0103291  
 Steidel C.C., Pettini M., Adelberger K.L., 2001, ApJ, astro-ph/0008283  
 Stern D., Djorgovski S.G., Perley R.A., de Carvalho R.R., Wall J.V., 2000, AJ, 119, 1526  
 Storrie-Lombardi L.J., Irwin M.J., McMahon R.G., Hook I.M., 2001, MNRAS, astro-ph/0012446  
 White R.L., Becker R.H., Helfand D.J., Gregg M.D., 1997, ApJ, 475, 479  
 White R.L., Becker R.H., Gregg M.D., Laurent-Muehleisen S.A., 2000, ApJS, 126, 133  
 Zheng W. et al, 2000, AJ, 120, 1607